# Spot Deformation and Replication in the Two-Dimensional Belousov-Zhabotinski Reaction in a Water-in-Oil Microemulsion

Theodore Kolokolnikov* and Mustapha Tlidi†

*Department of Mathematics and Statistics, Dalhousie University, Halifax, Canada*

*Optique Nonlinéaire Théorique, Université Libre de Bruxelles, Campus Plaine CP 231, 1050 Bruxelles, Belgium*

(Received 18 July 2006; published 3 May 2007)

In the limit of a large duffusivity ratio, spotlike solutions in the two-dimensional Belousov-Zhabotinski reaction in water-in-oil microemulsion are studied. It is shown analytically that such spots undergo an instability as the diffusivity ratio is decreased. An instability threshold is derived. For spots of small radius, it is shown that this instability leads to a spot splitting into precisely two spots. For larger spots, it leads to deformation, fingering patterns, and space-filling curves. Numerical simulations are shown to be in close agreement with the analytical predictions.

DOI: 10.1103/PhysRevLett.98.188303 PACS numbers: 82.40.Ck, 02.30.Jr, 02.60.Lj, 45.70.Qj

Localized patterns such as spots belong to the class of dissipative structures found far from equilibrium [1]. In recent years, considerable progress has been made in the understanding of these systems. The question of stability of such patterns is central, and the source of instabilities must be carefully scrutinized. In particular, the occurrence of instability can lead to the deformation of spots followed by spot multiplication (also called self-replication) or fingering. This intriguing phenomenon has been the subject of research since the pioneering work of Pearson [2]. Shortly after, thanks to the development of open spatial chemical reactors, self-replication was observed in various experiments such as ferrocyanide-iodate-sulphite reaction [3], the Belousov-Zhabotinsky reaction [4–6], and chloride dioxide-malonic-acid reaction [7]. By now, this phenomenon is believed to be universal [8,9]. It is not restricted to chemical reactions and occurs in many systems in biology [10], material science [11,12], and nonlinear optics [13].

Analytically, spot replication is relatively well understood in the one dimensional setting. Nishiura and Ueyama [14] proposed that self-replication of spikes occurs when the spike solution disappears due to the presence of a fold point. A similar explanation has been reported for the box-like patterns [15]. In two dimensions, a mechanism for spot instability has been proposed in [8] for general reaction-diffusion systems; related analysis was performed earlier in the framework of a piece wise-linear approximation in [16,17] and more recently in the context of diblock copolymer systems [11,12]. See also [18–20] and for a related approach from the point of view of interface motion.

In this Letter, we perform an analytical and numerical investigation of the two-dimensional localized spots that were recently reported for the Belousov-Zhabotinski (BZ) reaction in water-in-oil microemulsion [5,6]. In the classical BZ reaction, spiral waves are observed [21], but no localized spot solutions are possible. Indeed, localized structures develop only when the ratio of diffusion coefficients is sufficiently large, which occurs in the microemulsion system but not in the classical BZ reaction.

We consider the water-in-oil microemulsion model of the BZ reaction as described in [5,6]:

$$\varepsilon_0 v_t = \varepsilon_0 D_v \Delta v + [f_0 z + i_0(1 - mz)]\frac{v - q_0}{v + q_0} + \left[\frac{1 - mz}{1 - mz + \varepsilon_1}\right] v - v^2 \tag{1a}$$

$$z_t = D_z \Delta z - z + v\left[\frac{1 - mz}{1 - mz + \varepsilon_1}\right] \tag{1b}$$

where $v$, $z$ are dimensionless concentrations of activator $HBrO_2$ and oxidized catalyst $[Ru(bpy)_3]^{3+}$, respectively; $D_v$ and $D_z$ are dimensionless diffusion coefficients of activator and catalyst; $f$, $\varepsilon$, and $q$ are parameters of the standard Keener-Tyson model [21]; $i_0$ represents the photo-induced production of inhibitor; and $m$ represents the strength of oxidized state of the catalyst with $0 < mz < 1$. This reaction was shown experimentally and numerically to admit localized spot patterns that persist for a long time [5,6].

We rescale the variables as $z = 1/m - m^{-3/2} w \varepsilon_1$, $v = m^{-1/2}\hat{v}$, $t = \varepsilon_0 m^{1/2}\hat{t}$. In the new variables, after dropping the hats, we obtain

$$v_t = \varepsilon^2 \Delta v + f(v, w); \qquad \tau w_t = D\Delta w + g(v, w) \tag{2a}$$

where

$$f(v, z) = -[f_0 + f_1 w]\frac{v - q}{v + q} + \left[\frac{w}{1 + \alpha w}\right] v - v^2; \tag{2b}$$

$$g(v, w) = 1 - \left[\frac{w}{1 + \alpha w}\right] v \tag{2c}$$

and with the nondimensional constants given by

$$\alpha = m^{-1/2}, \quad f_1 = \varepsilon_1 m^{1/2}\left(i_0 - \frac{f_0}{m}\right), \quad q = q_0 m^{1/2}, \quad \varepsilon^2 = \varepsilon_0 D_v m^{1/2}, \quad D = D_z \varepsilon_1 m^{-1/2}, \quad \tau = \frac{1}{m}\frac{\varepsilon_1}{\varepsilon_0}. \tag{3}$$

In the limit $m \to \infty$, $f_1 \to 0$, and $\tau \to 0$, we obtain the

 

reduced system,

$$v_t = \varepsilon^2 \Delta v - f_0 \frac{v-q}{v+q} + wv - v^2$$
$$0 = D\Delta w + 1 - vw. \tag{4}$$

In particular, parameter values used in Fig. 14 of [6] are $f_0 = 2.18$, $i_0 = 0$, $m = 10$, $\varepsilon_1 = 0.01$, $\varepsilon_0 = 0.1$, and $D_z/D_v = 100$ which gives $\alpha = 0.3$, $f_1 = -0.007$, $\tau = 0.01$, so that the simplification (4) is appropriate.

Experimental and numerical evidence in [5,6] suggests that (1) admits localized spot solutions, such as shown in Fig. 1. Such spots occur in the regime where $\varepsilon \ll 1$. Our goal is to describe analytically the radius and profile of such a spot and then study its stability using singular perturbation techniques similar to those described in [8]. As we will demonstrate, the instability thresholds appear in the regime where $D \gg 1$. For sufficiently large values of $D$, a spot pattern is stable. However, as $D$ is decreased, instabilities of the form $\exp(\lambda t)\cos(m\theta)\phi(r)$ may develop, where $\theta$ and $r$ are the angular and radial coordinates, respectively. We provide the analytic description of the profile of the spot (7) and (10) and the dispersion relation (14) between $m$ and $\lambda$. This relation leads directly to the estimate for the instability threshold.

We begin by constructing a stationary (time-independent) spot-type solution on a two-dimensional unit disk $\{x:|x| < 1\}$. We assume that $D \gg 1$. Then to leading order, $w \sim w_0$ is a constant to be determined, and the solution for $v$ consists of an interface located at $|x| \sim l$ which connects two nearly spatially homogeneous layers. To find the profile of such an interface and its location $l$, let us rescale near $l$ as $v(x) = V(y)$ with $y = (r-l)/\varepsilon$ and $r = |x|$. For the steady state, we then obtain, to leading order, $V''(y) + f(V; w_0) = 0$. The interface solution corresponds to a heteroclinic orbit of this ODE. The existence of such an orbit is only possible whenever the equations

$$f(V_-; z_0) = 0 = f(V_+; w_0), \qquad \int_{V_-}^{V_+} f(s; w_0)\,ds = 0 \tag{5}$$

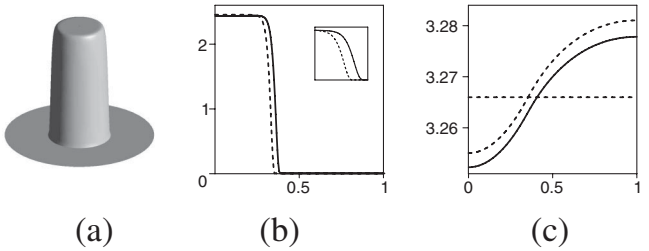


FIG. 1. (a) Radially symmetric, stable spot solution of the reduced BZ system (4) in the BZ system on a unit disk. (b) Radial profile of $v$ (solid curve) and its asymptotic approximation (dashed curves) given by (7). Insert: a blowup showing the profile of the interface. (c) Radial profile of $w$ (solid curve) and its two-term asymptotic approximations (dashed curves) given by (10). Parameter values are $D = 20$, $f_0 = 2.0$, $\varepsilon = 0.02$, $q = 0.005$.

are simultaneously satisfied for some values $V_- < V_+$. Since $q \ll 1$, we have $V_- \sim 0$, and (5) can be written as

$$f_0 + f_1 w_0 \sim \frac{3}{16}\left[\frac{w_0}{1+\alpha w_0}\right]^2; \qquad V_+ \sim \frac{3}{4}\left[\frac{w_0}{1+\alpha w_0}\right]. \tag{6}$$

Next, we ignore the $O(q)$ terms and integrate $V''(y) + f(V, w_0) = 0$ to obtain

$$v \sim \begin{cases} V_+ \tanh^2\left[\sqrt{\frac{V_+}{6}}\left(\frac{r-l}{\varepsilon}\right)\right], & r < l \\ 0, & r > 0 \end{cases} \tag{7}$$

with $V_+$ and $w_0$ given by (6) and where $r = |x|$. This formula describes the profile of the interface in the limit $q \to 0$. Its thickness is of $O(\varepsilon V_+^{-1/2})$. To determine its location $l$, we integrate the second equation in (2a). Zero-flux conditions then yield $\int g = 0$ so that

$$g(V_+, w_0) l^2 + (1-l^2) g(0, w_0) \sim 0. \tag{8}$$

In the limit of the reduced system (4), we obtain

$$l \sim \frac{1}{2\sqrt{f_0}}, \qquad w_0 \sim \frac{4}{\sqrt{3}}\sqrt{f_0}, \qquad V_+ \sim \sqrt{3 f_0}. \tag{9}$$

To determine the correction to $w$, we write $w = w_0 + D^{-1} w_1 + O(D^{-2})$ to obtain $\Delta w_1 + g(w_0, v_0) = 0$. Imposing continuity at the interface $r = l$, the solvability condition $w_1(l) = 0$, and using (8) and $g(0, w_0) = 1$, we then obtain

$$w \sim w_0 + \frac{1}{4D}\begin{cases} -\dfrac{(1-l^2)(l^2-r^2)}{l^2}, & r < l \\ 2\ln\left(\dfrac{r}{l}\right) + l^2 - r^2, & r > l \end{cases}. \tag{10}$$

An example of a localized spot and its radial profile is shown in Fig. 1.

When decreasing the diffusion coefficient $D$ of the recovery variable, numerical simulations show that the spot becomes unstable. To compute the threshold associated with this instability, we linearize around the localized spot solution (7) as

$$v(x, t) = v(x) + \exp(\lambda t)\cos(m\theta)\phi(r)$$
$$w(x, t) = w(x) + \exp(\lambda t)\cos(m\theta)\psi(r)$$

where $v$ and $w$ are given to leading order in (7) and (9), $m$ is an integer, $\phi, \psi \ll 1$ and $(r, \theta)$ are the polar coordinates of $x$. Substituting into (1), we then obtain

$$\lambda\phi = \varepsilon^2\left(\phi_{rr} + \frac{1}{r}\phi_r - \frac{m^2}{r^2}\phi\right) + f_v\phi + f_w\psi \tag{11a}$$

$$\tau\lambda\psi = D\left(\psi_{rr} + \frac{1}{r}\psi_r - \frac{m^2}{r^2}\psi\right) + g_v\phi + g_w\psi. \tag{11b}$$

Note that $v_r$ satisfies that $\varepsilon^2(v_{rrr} + 1/r v_{rr} - 1/r^2 v_r) + f_v v_r + w_r f_w = 0$. Therefore, multiplying (11b) by $v_r$ and integrating by parts, we obtain

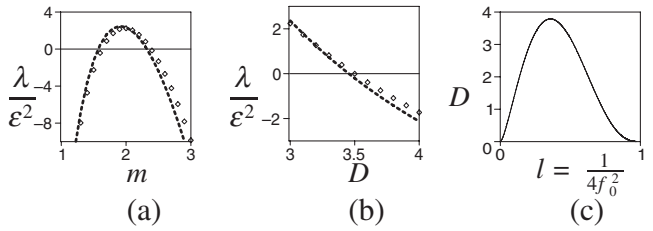


FIG. 2. (a), (b) Comparison of numerical computations of $\lambda$ given by (11) (diamonds) with the analytical result (14) and (16) (dashed line) for the reduced model (4) on a unit disk. Parameter values are $q = 0.01$, $\varepsilon = 0.01$, and (a) $D = 3, f_0 = 1.3$; (b) $m = 2, f_0 = 1.3$. (c) Simultaneous solution of $\lambda = 0 = d\lambda/dm$, showing the first value of $D$ for which instability occurs. The system is stable above the curve and unstable below it. To compute $\lambda$ numerically, (11) was reformulated as a boundary value problem by adjoining the equation $d\lambda/dr = 0$ along with fixing $\psi(1)$. Maple's numerical boundary value problem solver was then used with initial guesses $\phi = v_r$, $\lambda = 0$, and $\psi =$ the solution of (13). All computations are correct to four significant digits.

$$\left(\lambda + \frac{(m^2-1)\varepsilon^2}{l^2}\right)\int v_r^2 \sim \int v_r f_w(\psi - w_r) \qquad (12)$$

where we have assumed that to leading order, $\phi \sim v_r$, $\lambda \ll 1$, $\psi \ll \phi$. Since $v_r$ is exponentially small outside the interface, we simplify $\int v_r f_w(\psi - w_r) \sim -[\psi(l) - w_r(l)] \times \int_0^{V_+} f_w(v, w_0)dv$. We estimate $w_r(l) \sim -1/(2D)g(V_+, w_0)$ and to determine $\psi(l)$, we integrate (11b) over the interface $l$ to obtain $D\psi_r|_{l^-}^{l^+} \sim -g(0, w_0)/l^2$ where we have used $\phi \sim v_r$ and (8). Keeping only leading order terms in $D$, we then obtain the following problem for $\psi$:

$$0 = \psi_{rr} + \frac{1}{r}\psi_r - \frac{m^2}{r^2}\psi = 0, \qquad r \neq l \qquad (13a)$$

$$\psi'(0) = 0 = \psi'(1), \qquad \psi'(l^+) - \psi'(l^-) = -\frac{1}{Dl^2}g(0, w_0). \qquad (13b)$$

Using the continuity of $\psi$ at $r = l$, we get

$$\psi(l) \sim \frac{1}{2Dml}g(0, w_0)(1 + l^{2m})$$

and substituting into (12), we obtain

$$\lambda\frac{l^2}{\varepsilon^2} \sim 1 - m^2 + A\left[1 - l^2 - \frac{1}{m}(1 + l^{2m})\right] \qquad (14)$$

where

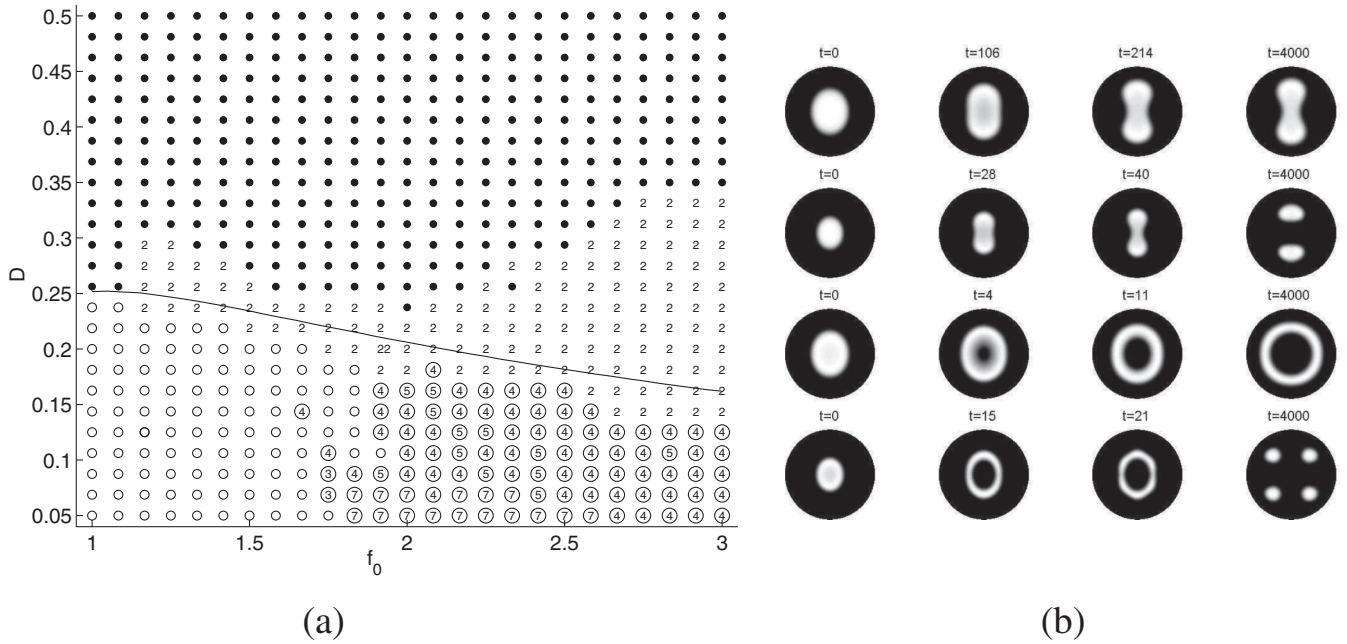


FIG. 3. (a) Bifurcation diagram for (4) in $D$ and $f_0$ with $\varepsilon = 0.05$, $q = 0.01$. Solid dots represent deformations of a spot without topological change. Points marked by "2" represent spot-replication into two spots. An empty circle represents spot-to-ring bifurcation and an empty circle with a number inside represents spot-to-ring-to-spots bifurcation. A solid line represents the boundary of spot-to-ring replication which occurs at the fold point of the radially symmetric steady state. The bifurcation diagram was obtained by solving the full two-dimensional system (4) using the finite element package FLEXPDE [23] with zero-flux boundary conditions and 800 elements on a quarter-disk. For initial conditions, (7), (9), and (10) was used, but with $r$ replaced by $r(1 + 0.05\cos 2\theta)$. The solid line was obtained by solving for the fold point of the radially symmetric steady state using Maple's boundary value problem solver. (b) Full numerical simulations starting from a spot-state (7) and (10) as initial conditions. First row: spot deformation, $f_0 = 1.3$, $D = 0.35$. Note that the final steady state of the system is a deformed blob shown here at $t = 4000$. Second row: self-replication, $f_0 = 2.2$, $D = 0.24$. Third row: spot-to-ring bifurcation, $f_0 = 1.3$, $D = 0.1$. Fourth row: spot-to-ring-to-spots bifurcation, $f_0 = 2.6$, $D = 0.1$.

$$A = \frac{l}{2\varepsilon D}\frac{g(0,w_0)[\int_0^{V_+} f_w(v,w_0)dv]}{\varepsilon \int v_r^2}. \quad (15)$$

For the reduced model (4), we obtain an explicit result

$$A \sim \frac{3^{5/4}2^{1/2}5}{64}\frac{1}{f_0^{3/4}\varepsilon D} = 0.43622\frac{1}{f_0^{3/4}\varepsilon D}. \quad (16)$$

In Fig. 2, the analytical prediction given by (14) is found to be in good agreement with the numerical computations of problem (11). Full numerical simulations of (4) also agree with this prediction. For example, when taking $\varepsilon = 0.03$, $f_0 = 1.3$ and $q = 0.01$, slight spot deformation corresponding to mode $m = 2$ is observed when $D = 1.0$ but not when $D = 1.3$. This agrees well with $D \sim 1.1$, the threshold predicted by (14).

From (14) and (16), it is clear that the mode $m = 1$ is always stable and that for large enough $D$, all modes $m \geq 1$ are stable. As $D$ is decreased, instability sets in when $D = O(\varepsilon^{-1})$. The threshold value is found by simultaneously solving $\lambda = d\lambda/dm = 0$. The resulting graph is shown on Fig. 2(c). In particular, note that the system is stable if $D\varepsilon > 0.038$, independent of the value of $f_0$. In the limit of small radius $l \to 0$, the first unstable integer mode is $m = 2$ corresponding to $A = 6$, so that the spot of small radius becomes unstable whenever $\varepsilon D f^{3/4} \leq 0.0727$. More generally, by eliminating $A$, we find that there exist constants $l_1 < l_2 < \ldots < 1$ such that the first unstable mode is $m$ provided that $l_{m-1} < l < l_m$, where $l_1 = 0$, $l_2 = 0.491$, $l_3 = 0.667$, $l_4 = 0.753$, and $l_m \sim 1 - 0.937/m$ as $m \to \infty$, where 0.937 is the root of $e^{-2z}(3 + 2z) + 3 - 4z = 0$.

Numerical computations indicate that self-replication is more prevalent for spots of small radius (see Fig. 3). For larger spots, a deformation usually leads to the so-called ''finger growth'' and space-filling curves. Others studies have shown the occurrence of fingering instabilities leading to labyrinthine patterns [8,18,22]. The question of whether the self-replication or fingering instability occurs first is still open.

For smaller, $O(1)$ values of $D$, there is also a different instability mechanism that can lead to splitting of a spot into a ring as illustrated in Fig. 3. Unlike spot multiplication, this instability is radially symmetric and is caused by the *disappearance* of the steady state solution—whereby the steady state solution ceases to exist due to the presence of a saddle-node bifurcation—rather than by its lateral instability. Numerical simulations suggest that spot replication occurs only for spots of smaller radius, whereas spot-to-ring instability is dominant for larger spots.

To conclude, we have estimated analytically for which value of diffusion $D$ spot deformation first occurs. As $D$ is decreased further, self-replication and/or spot-to-ring instability is observed. As evidenced by numerical simulations, we conjecture that spot deformation is the precursor to this phenomenon.

The authors are grateful to Vladimir Vanag and Irving Epstein for introducing us to this subject and for illuminating discussions. We are also grateful to the anonymous referees whose suggestions have improved the paper significantly. T. K. is supported by NSERC Canada. M. T. is supported by the FNRS Belgium.

*Electronic address: tkolokol@mathstat.dal.ca
†Electronic address: mtlidi@ulb.ac.be

[1] P. Glansdorff and I. Prigogine, *Thermodynamic Theory of Structures, Stability and Fluctuations* (Wiley, New York, 1971); E. Meron, Phys. Rep. **218**, 1 (1992); J. Chanu and R. Lefever, Physica A (Amsterdam) **213**, xiii (1995); M. C. Cross and P. C. Hohenberg, Mod. Phys. Lett. A **65**, 851 (1993); R. Kapral and K. Showalter, *Chemical Waves and Patterns* (Kluwer Academic press, Dordercht, 1995).
[2] J. E. Pearson, Science **261**, 189 (1993).
[3] K. Lee, W. D. McCormick, J. E. Pearson, and H. L. Swinney, Nature (London) **369**, 215 (1994).
[4] A. P. Muñuzuri, V. Pérez-Villar, and M. Markus, Phys. Rev. Lett. **79**, 1941 (1997).
[5] A. Kaminaga, V. K. Vanag, and I. R. Epstein, Angew. Chem. **45**, 3087 (2006).
[6] A. Kaminaga, V. K. Vanag, and I. R. Epstein, J. Chem. Phys. **122**, 174706 (2005).
[7] P. W. Davis, P. Blanchedeau, E. Dulos, and P. De Kepper, J. Phys. Chem. A **102**, 8236 (1998).
[8] C. Muratov and V. V. Osipov, Phys. Rev. E **53**, 3101 (1996); **54**, 4860 (1996); C. Muratov, Phys. Rev. E **66**, 066108 (2002).
[9] Y. Hayase and T. Ohta, Phys. Rev. Lett. **81**, 1726 (1998); Y. Hayase, Phys. Rev. E **62**, 5998 (2000).
[10] E. Meron, E. Gilad, J. von Hardenberg, and M. Shachak, Chaos Solitons Fractals **19**, 367 (2004).
[11] X. Ren and J. Wei, SIAM J. Math. Anal. **35**, 1 (2003).
[12] Y. Nishiura and H. Suzuki, SIAM J. Math. Anal. **36**, 916 (2004).
[13] M. Tlidi, A. G. Vladimirov, and P. Mandel, Phys. Rev. Lett. **89**, 233901 (2002).
[14] Y. Nishiura and D. Ueyama, Physica D (Amsterdam) **130**, 73 (1999).
[15] T. Kolokolnikov, M. Ward, and J. Wei, arXiv:nlin/0701053 [Physica D (to be published)] ;B. S. Kerner and V. V. Osipov, *Autosolitons: A New Approach to Problems of Self-Organization and Turbulence* (Kluwer, Dordrecht, 1994).
[16] T. Ohta, M. Mimura, and R. Kobayashi, Physica D (Amsterdam) **34**, 115 (1989).
[17] S. Kawaguchi and M. Mimura, SIAM J. Appl. Math. **59**, 920 (1999).
[18] R. E. Goldstein, D. J. Muraki, and D. M. Petrich, Phys. Rev. E **53**, 3933 (1996).
[19] C. B. Muratov, Phys. Rev. E **54**, 3369 (1996).
[20] D. Gomila, P. Colet, G. L. Oppo, and M. San Miguel, Phys. Rev. Lett. **87**, 194101 (2001).
[21] J. J. Tyson and P. Fife, J. Chem. Phys. **73**, 2224 (1980); J. P. Keener and J. J. Tyson, Physica D (Amsterdam) **21**, 307 (1986).
[22] K. Lee and H. Swinney, Phys. Rev. E **51**, 1899 (1995).
[23] See FLEXPDE website, www.pdesolutions.com.